Adsorption, 1, 153–164 (1995)

Radial Flow Rapid Pressure Swing Adsorption

A.S.T. CHIANG* AND M.C. HONG
Department of Chemical Engineering, National Central University, Chung-Li, Taiwan, ROC 32054

Received January 4, 1994; Revised June 28, 1994; Accepted July 14, 1994

Abstract. A new PSA process has been proposed and experimentally verified. This process was operated with a radial flow geometry under a cycle time less than 30 seconds. It has been showed that enriched oxygen could be produced when air was fed inward. The same system showed virtually no separation effect if the feed direction was reversed. The change of separation efficiency upon flow reversal was most significant when small adsorbent particles were employed. A ϕ 200 × 75 mm annular packing with 3 μm particles of zeolite 5A was able to produce 60% purity oxygen from air. The effect of flow direction on system performance confirmed the importance of flow resistance distribution. In radial flow geometry, most of the flow resistance was located near the center of the disk. The relative small pressure gradient at the feed end enabled a better absorbent utilization during the inward feed step, and a more effective desorption during the vent step. The same principle could be extended to other geometric configurations.

Keywords: bulk separation, pressure swing adsorption, radial flow chromatography, air separation, oxygen enrichment, zeolite 5A

Introduction

Pressure swing adsorption (PSA) process has, in the past thirty years, gained increasing applications in the gas separation industry. To date, PSA processes based on either adsorption equilibrium or adsorption kinetics can be found. Its design ranges from the simple dual bed process for air drying to the complicated multi-bed processes for the fractionation of gas mixtures (Kumar et al. 1992).

A special variation of PSA process, Rapid Pressure Swing Adsorption (RPSA), was proposed by Jones and Keller in 1980. The RPSA process was operated with a cycle time less than 1 minute as compared to the 2 to 3 minutes normally required in conventional PSA processes. The rapid swing of inlet pressure in a RPSA process was in some sense similar to the earlier design of Turnock and Kadlec (1971) and Kowler and Kadlec (1972) on parametric pump. Turnock and Kadlec, however, had operated their system with a cycle time of about 3 seconds. While Turnock and Kadlec used two steps (adsorption and desorption) of equal length, a RPSA cycle usually included three steps of different duration's. The RPSA process was particularly good for small systems and generally displayed to a higher productivity than the conventional system. It has become the standard unit used in portable oxygen generators. However, despite the commercial success of RPSA cycles, surprisingly few theoretical investigation has been published. The work of Doong and Yang (1988) was one of the exceptions.

Changing the packed column configuration commonly used is PSA processes to a radial flow geometry has been strongly advocated by Rota and Wankat (1991). They argued that, based on their earlier theoretical study (Rota and Wankat 1990) on the scaling and intensifying of PSA processes, the performance of both axial and radial flow PSA processes would be identical if equilibrium theory prevails. The radial flow geometry, however, had the extra benefit of large cross-section area, small pressure drop and the ease to scale up.

The scaling rules of Rota and Wankat (1990) were originally derived to compare the productivity of the same PSA process under different unit sizes. They have found that the productivity could be improved if a shorter bed (or thinner shell in the radial flow case) of smaller adsorbent particles were employed under a faster cycle. In practice, the cycle time was limited by the mass transfer rate into the adsorbents. With smaller particle size, the mass transfer rate could be

*To whom the correspondence should be addressed.

accelerated, but at the same time the pressure drop across the bed would be enlarged. A shallow bed must thus be employed to compensate the higher flow resistance of smaller particles. A radial flow configuration with a thin shell of adsorbent could be scaled up much easier than a flat shallow bed.

As mentioned earlier, the RPSA process was indeed operated under a rather fast cycle. This seemed to go in hand with the suggestion of Rota and Wankat. There was but a completely different reason for the success of RPSA processes. The scaling rules of Rota and Wankat had been derived assuming the normalized concentration profiles could be kept identical in spite of the geometry change. This assumption could not hold if a significant pressure drop existed in the system. The RPSA process, on the contrary, capitalized on the pressure drop across the bed. In fact, a major effort has been to select the optimum particle size that created enough pressure drop while still meeting the necessary throughput.

According to the analysis of Doong and Yang (1988), a RPSA air separation process could not be operated without flow resistance. A reasonable pressure drop must be kept to prevent the feed from penetrating the adsorption bed. As a consequence, the adsorbent utilization would be relative low. The pressure drop was however, beneficial to the desorption step. The lower pressure end had a chance to desorb more thoroughly before the purge gas arrived. In other words, the effects of pressure drop were different during the adsorption and desorption steps.

Radial Flow Rapid PSA

Will there be any advantage if one changes a RPSA process to a radial flow geometry? This can not be answered directly from the analysis of Rota and Wankat, where they have precluded the effect of pressure drop. When there is a significant pressure drop, the concentration and pressure profiles will be very different in radial and axial flow systems.

A qualitative sketch of the pressure profiles along the flow direction under a constant volumetric flow rate has been demonstrated in Fig. 1. An axial flow geometry led to a nearly constant pressure gradient along the flow direction. In radial geometry, however, the pressure drop increased quickly with a decreasing radius due to the reduced cross sectional area. As a result, there was a steep gradient located at the center. This steep gradient would be at the outlet if the gas was flowing inward, and at the inlet if the flow direction was reversed. Furthermore, for the same volume of packing, a radial flow arrangement would give a smaller total pressure drop due to a larger cross sectional area. The pressure profiles in this figure have been normalized to emphasize only the distribution of resistance.

The uneven distribution of pressure gradient suggested some possible benefits for a Radial Flow RPSA process. If high pressure gas was fed from outside, the pressure wave might travel deeper into the packing than the axial case without feed breakthrough. A large portion of the adsorbents would then be exposed to the feed pressure, and the adsorbent utilization could be improved. During the vent step, pressure at the less resistive feed end could be reduced quickly. The desorption rate would thus be accelerated.

The analyses above have of cause neglected the transient movement of pressure wave, as well as the complication of varying flow rate due to adsorption and desorption. For an air separation process, the gas flow rate decreased dramatically along the direction of feed. For a typical system that produce 90% oxygen at 30% recovery, only 7% of the feed gas actually reached the outlet. The remaining part of the feed was adsorbed along the way. Therefore, during the adsorption step of an axial flow system, the pressure gradient would be steeper behind the concentration wave due to its higher velocity. The penetration of pressure wave could not be deep. Most of the adsorbent was never given high enough pressure to fully utilize its capacity.

The changing cross sectional area in a radial geometry turns out to accommodate the reduce flow rate perfectly. When fed from outside, a high flow rate is met by a large cross sectional area. The cross sectional area continuously decreases with decreasing radius, while the flow rate also reduces by adsorption. The local gas velocity may depend on the rate of adsorption, but the pressure gradient near the inlet will certainly be smoother than in the axial flow case. At the end of adsorption step, there will be an annular section at relative higher pressure.

The conceivable history of pressure profile during a Radial Flow RPSA cycle has been suggested in Fig. 2. It was compared with the change of column pressure profile given by Keller and Jones (1980). More adsorbent would experience a larger pressure swing in a radial flow geometry than in an axial flow case. However, to theoretically assess the possible productivity gain in a radial flow geometry, one would have to solve a very complicated model. Therefore, this proposal was directly tested by experiments instead.

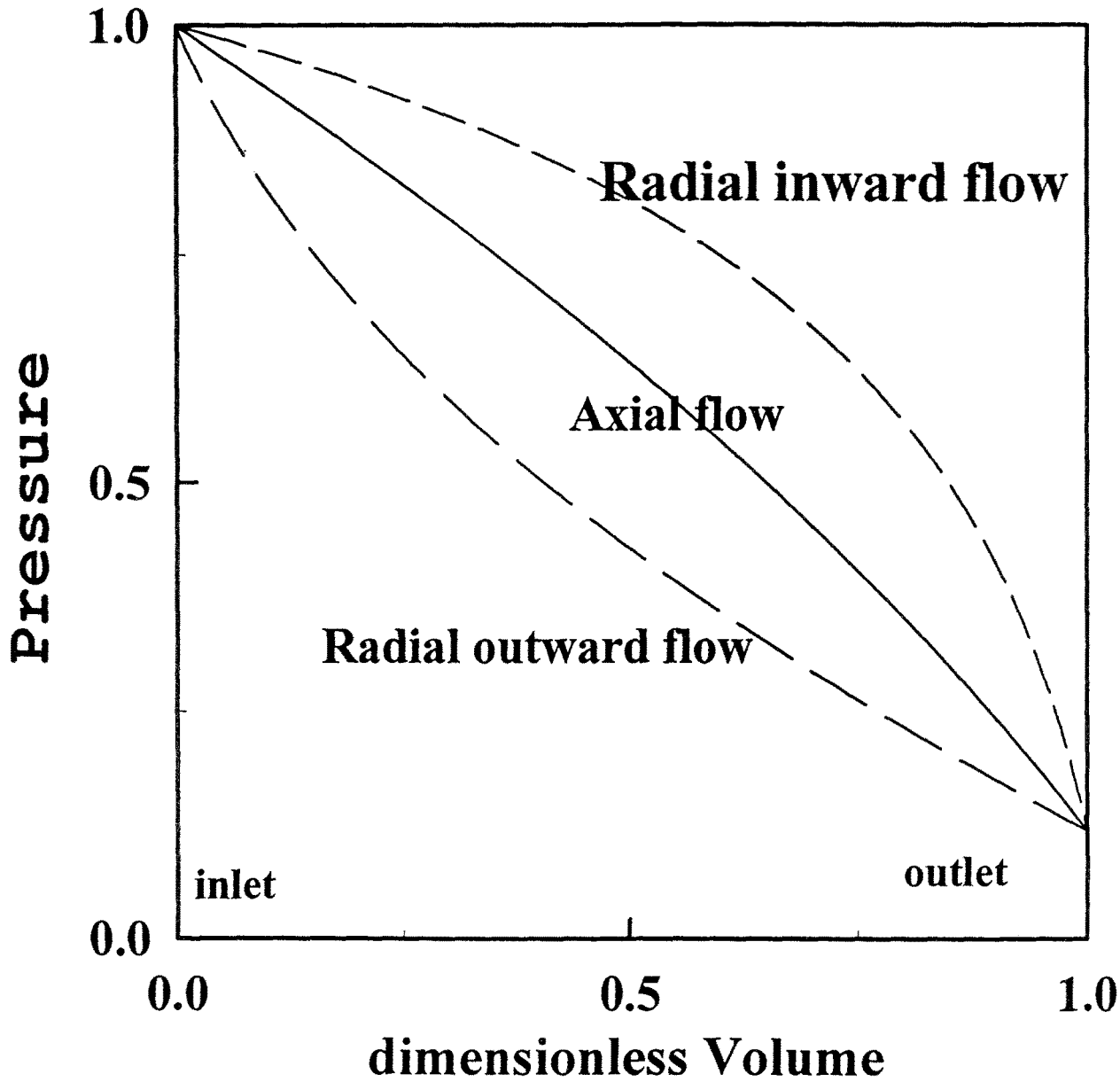

Fig. 1. Qualitative sketch of the pressure profiles under constant volumetric flow rate along the flow direction in an axial flow configuration and in two different radial flow configuration.

Experimental Radial-Flow-Rapid-PSA (RFRPSA) System

The design of our experimental RFRPSA system has been sketched in Fig. 3. It was basically the same system we have employed earlier to study an axial flow rapid PSA process (Wu 1992). The only change made was the replacement of adsorption column with a disk-shape container. The design of the container and its dimension were given in Fig. 4.

Commercial zeolite 5A pellets (UOP, lot no. 93191080029) crashed and screened to specified sizes were packed into a 75 mm high annular basket and placed in the container. The basket was made of fine gauged stainless steel screen, with an outer diameter of 200 mm and a 22 mm diameter hole in the center.

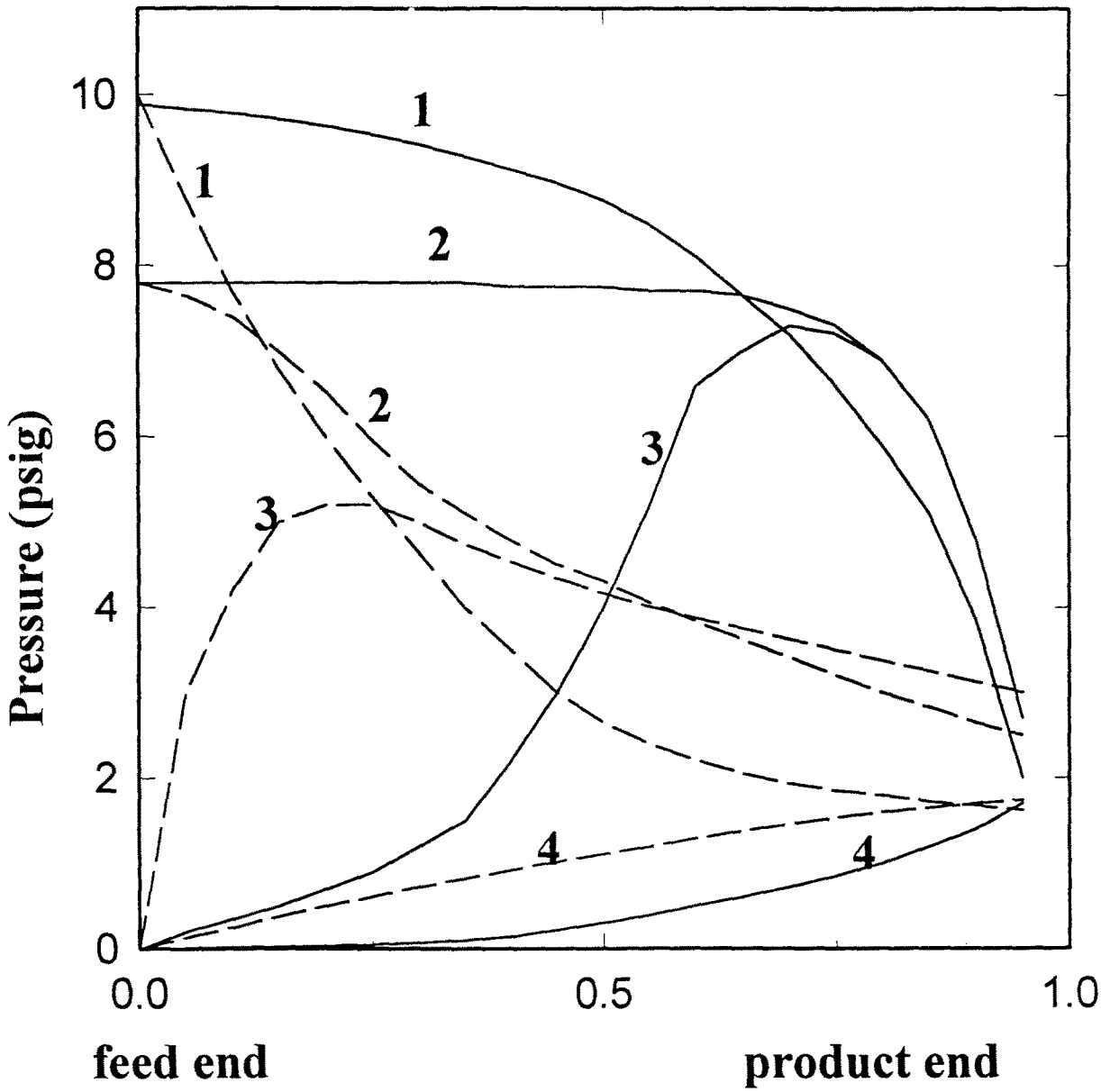

Fig. 2. The pressure profiles along the feed direction during an axial RPSA cycle and an inward feed radial RPSA cycle. The dashed lines are for the axial flow case (after Keller and Jones 1980). The solid lines are for radial flow case. 1, middle of feed step; 2, middle of delay; 3, early in exhaust; 4, last in exhaust.

Roughly 600 gm of zeolite particles could be packed into this basket. The zeolites were activated at 300°C in an open oven for one day prior to packing. Several layers of rubber gasket were put above and below the basket. By tightening the screws on the container, these gaskets were compressed on the basket so that leakage could be minimized. The packed particles were also compressed by the same action. However, these particles might rearrange themselves during the following rapid swing of pressure. A lost of pressure drop was noticed if the same packing was operated for a long time. We had to add more layers of rubber to eliminate this channeling problem if this happened.

Silica gel particles were employed to reduce the dead volume at places such as the clearance between the basket and the container, the center hole and the concentric

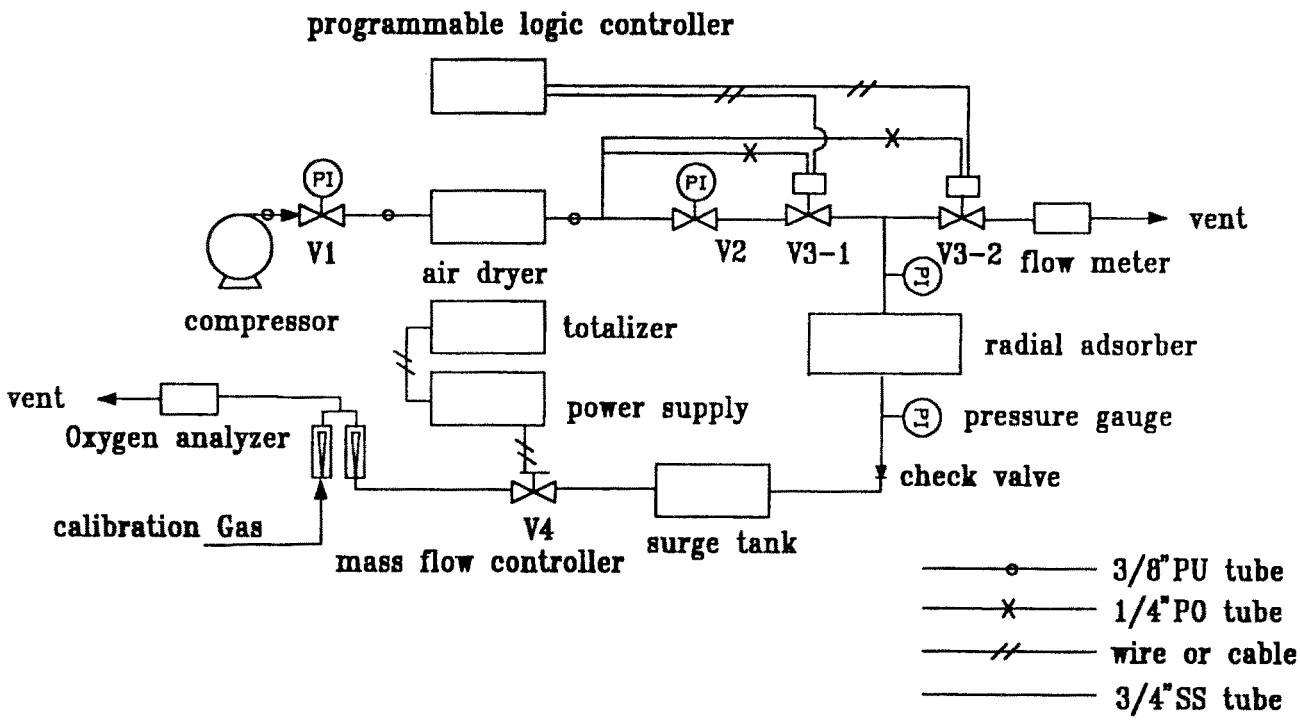

Fig. 3. Schematics of the experimental system and apparatus.

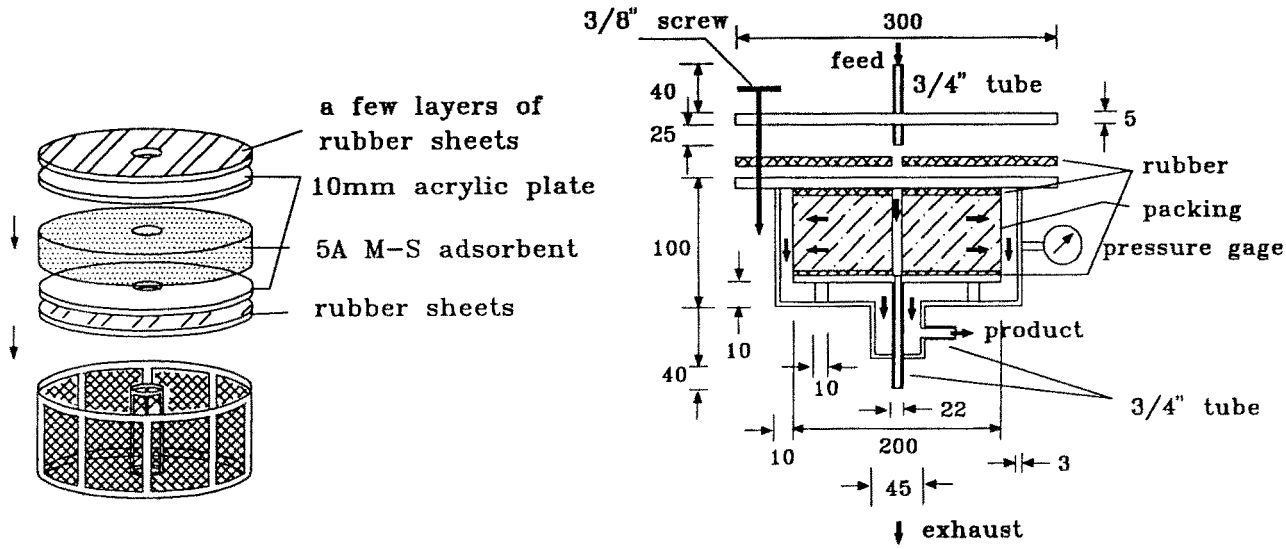

Fig. 4. The dimensions and design of the annular basket and the container for a radial flow packing. The feed and product end can be reversed by changing the pipings.

tubing section. Besides this purpose, the silica gel also served as a flow distributor and a drying add to the feed air. Powders of Zeolite 5A (log # 943090060196) have also been employed as the absorbent. For these fine powders (about 3 μm) we have to added a layer of non-woven cloth next to the stainless steel screen to prevent the powder from blowing downstream.

Compressed air, passing through a bed of silica gel to remove the moisture, was regulated to 20 psig and fed to the packed disk through an air actuated switching

valve. The valve was controlled by a programmable logical controller. Two flow arrangements, either inward or outward feed, were tested. Product gases, passing in series through a check valve, a surge tank roughly 800 cm^3 in size, and a mass flow controller (Brook 5080 USA), went to the oxygen analyzer (Teledyne 320 P/D USA). This oxygen analyzer had a 0.5% sensitivity of the full range, but it did not respond to argon. The blowdown gas was directed to a dry gas meter (STEC SEF-51 Japan). We did not measure the amount of air fed to the system since it could be obtained from a material balance.

Results and Discussions

Three types of particle sizes, 60/80 mesh, 200/325 mesh particles and the 3 μm powder, have been studied. The cycle time varied from 2 to 20 seconds, with different duration's for the feed, delay and vent steps. Showed in Fig. 5 were the product oxygen purity and recovery when the 60/80 mesh particles were used. The open symbols represented the results of outward feed operations. The solid symbols were for the inward feed operations. The number in the figure indicated the production rate in cc/min. For these runs, the feed plus the delay time varied from 1 to 2 seconds. The total cycle time was 6 to 8 seconds for the inward feed operations, and 12 to 20 seconds for the outward feed cases. This was because a larger feed flow rate could be attended under inward feed condition for the same pressure setting. The outward feed operation also required a much longer exhaust step to vent.

There were only a few percentages of product oxygen enrichment obtained with 60/80 mesh packing, no matter which direction had the air been feed. The inward feed operations gave just slightly better result than the outward feed cases. The recovery was also extremely low within the range of cycle times studied. Since the pressure drop across a 90 mm radius was practically zero in these cases, it could have been analyzed with the model of Rota and Wankat. Both the inward and outward feed operations acted just as a shallow bed. Neither the feed direction nor the axial or radial configurations made any difference.

From the pressure variation at the product end, it was also certain that the pressure wave had passed through the packed section into the surge tank. One would have to reduce the feed time to a fraction of a second to prevent breakthrough, which was beyond the response time of our control valve.

In Fig. 6, results of the same system with 200/325 mesh (about 60 μm) packing were illustrated. The feed times in this case varied from 2 to 5 seconds. The delay times ranged from 1 to 3 seconds. For the outward feed operations the vent step was 16 to 20 seconds, while it was 12 to 18 seconds for inward feed cases. With feed going outward (open symbols), a smaller particle size made little improvement on the product purity compared to the previous case. A better recovery was however achieved due to less feed gas admitted under a higher flow resistance. The inward feed operation (solid symbols), on the other hand, enjoyed a substantial increase of product purity by changing from 60/80 to 200/325 mesh particles. A product oxygen purity of 35% was accomplished at a recovery of 5%. The fact that a large difference in product purity was generated by a simple reversal of flow direction, confirmed the importance of flow resistance distribution. It further implied that the axial flow system, which had a resistance distribution in between the two radial operational modes, should have an outcome bounded by the results of two radial modes.

The performance gap between the two radial operational modes become even wider when 3 μm powders were employed. As illustrated in Fig. 7, the product gas contained now approximately 50% to 60% oxygen when feeding from outside. The maximum oxygen purity obtained in the reversed direction was only 27%. The recovery in both cases was however still low.

The cycle times employed in the 3 μm packing experiments were listed in Tables 1 and 2, along with the pressure ranges observed at the product end and the surge tank. With these small particles, pressure drop was significant. Moreover, the pressure drop experienced during outward feed operation was about three times that during the reversed operation. The amount of feed gas entered was thus five time smaller in the former case.

During the inward feed operation, distinct pressure swing was experienced at the product end. The maximum pressure here increased from 10 to 15 psig when the feed step changed from 3 to 6 seconds. This suggested that the pressure wave had reached the product end in about 4 seconds, whereas a vent step of 10 to 14 seconds was needed to release the product end pressure to 4 psig. For the outward feed operation, the product end pressure never exceeded 10 psig even with prolonged feed step, and 20 seconds of exhaust time was needed to vent the desorbed gas.

In Table 3, representative data on RPSA cycles reported by different researchers were summarized along

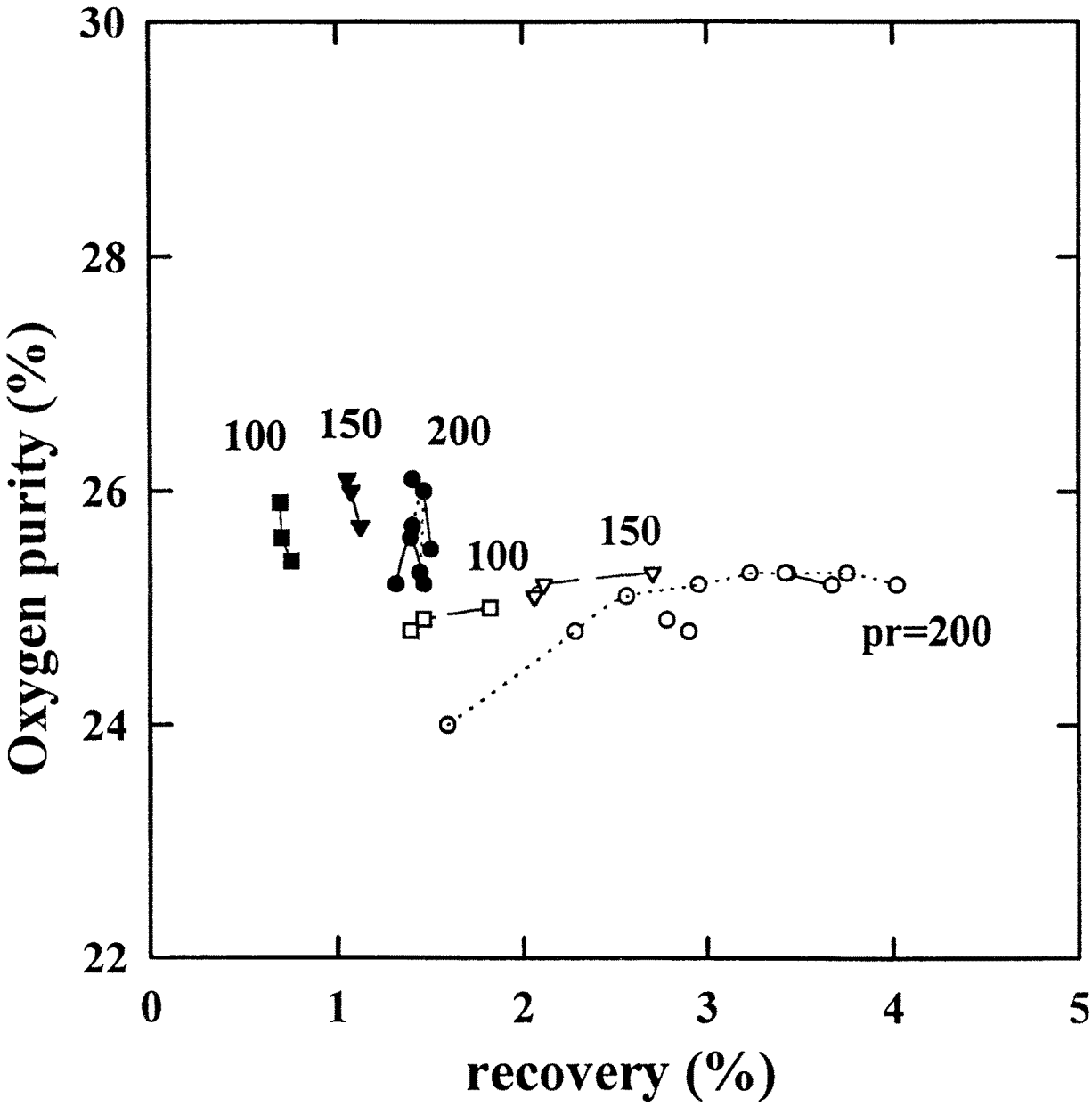

Fig. 5. The performance of the radial flow RPSA system with 60/80 mesh 5A particle packing. The open symbols are for outward feed, the solid symbols are for inward feed. Numbers indicated are the production rates in cc/min. The data were collected with different step durations. The feed pressure was all 20 psig.

with our results. All previous studies were conducted with packed columns. Different column lengths have been examined with feed pressure ranged from 10 to 50 psig. The data of Wu (1993) was particular worth mentioned because it had been conducted in our laboratory with the same adsorbent on the same apparatus, except for the packing configuration.

The column length, particle size, step duration, as well as feed and product pressure were all important factors to the results of a RPSA process. The data showed in Table 3 have been selected to indicate the highest productivity and purity attainable in each study. In general, product purity and recovery increased with column length and feed pressure. For longer column, a

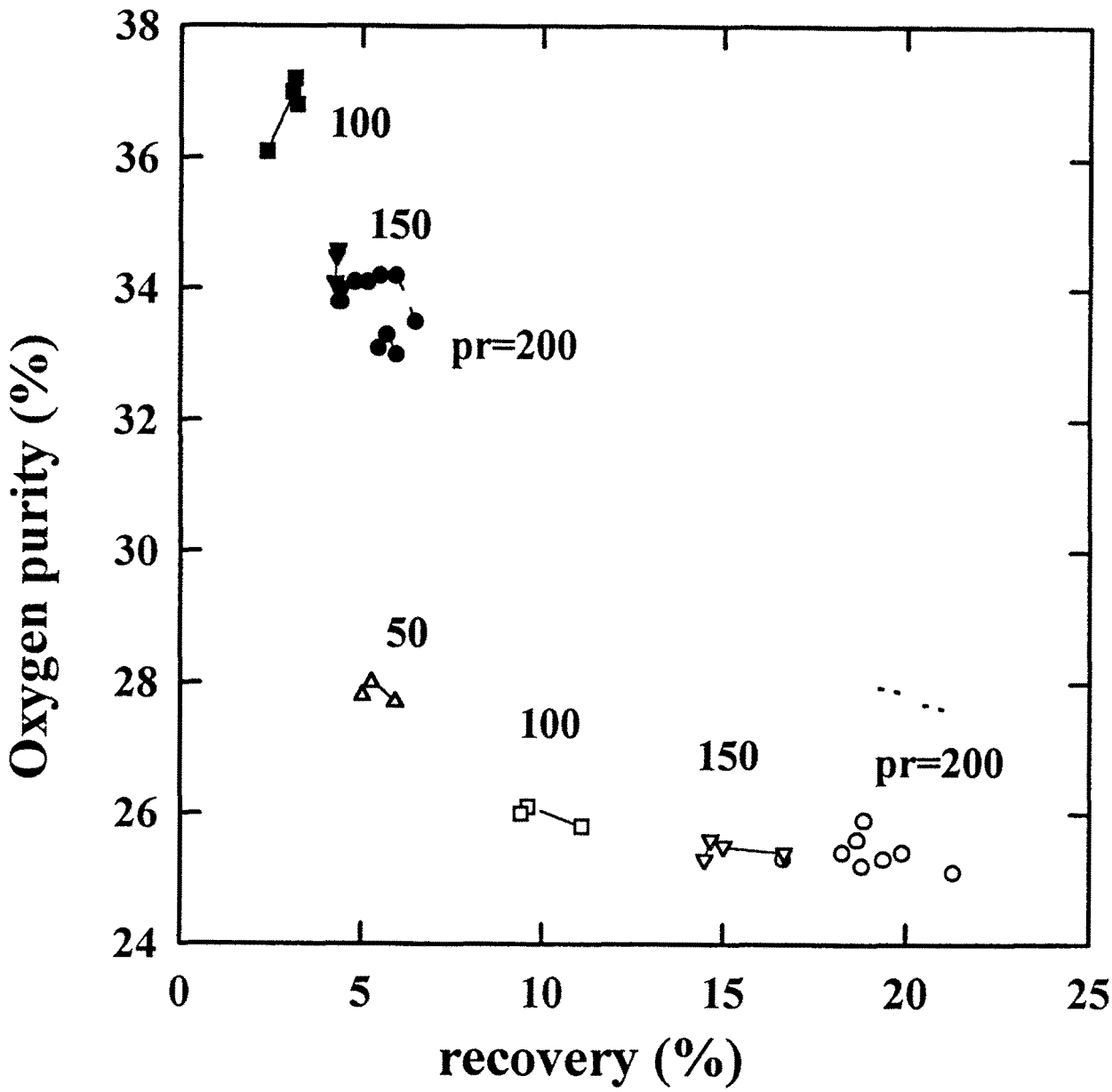

Fig. 6. The performance of the RFRPSA system with 200/325 mesh 5A particle packing. The notations are the same as in Fig. 5.

higher feed pressure and extended exhaust time must be employed. Product with better than 90% oxygen purity was only possible with columns longer than 30 cm. Below this length, the feed time must be reduced to a fraction of a second to avoid the breakthrough of nitrogen. If it was not possible to do so, only oxygen enriched gas could be produced.

The first impression from this table seemed to suggest that our radial flow system was inferior to the column operations in both the recovery and the product purity. However, the depth of adsorbent in our radial configuration was only 9 cm, while the reported studied had at least 23 cm in packing depth. We believed that a result better than those of Wu's should be feasible had the packing depth been the same. Conversely speaking, a product purity of 55% would not be possible with a 9 cm column.

One might wonder that an increase of packing radius could result into a serious pressure drop and block the gas flow completely. The magnitude of pressure

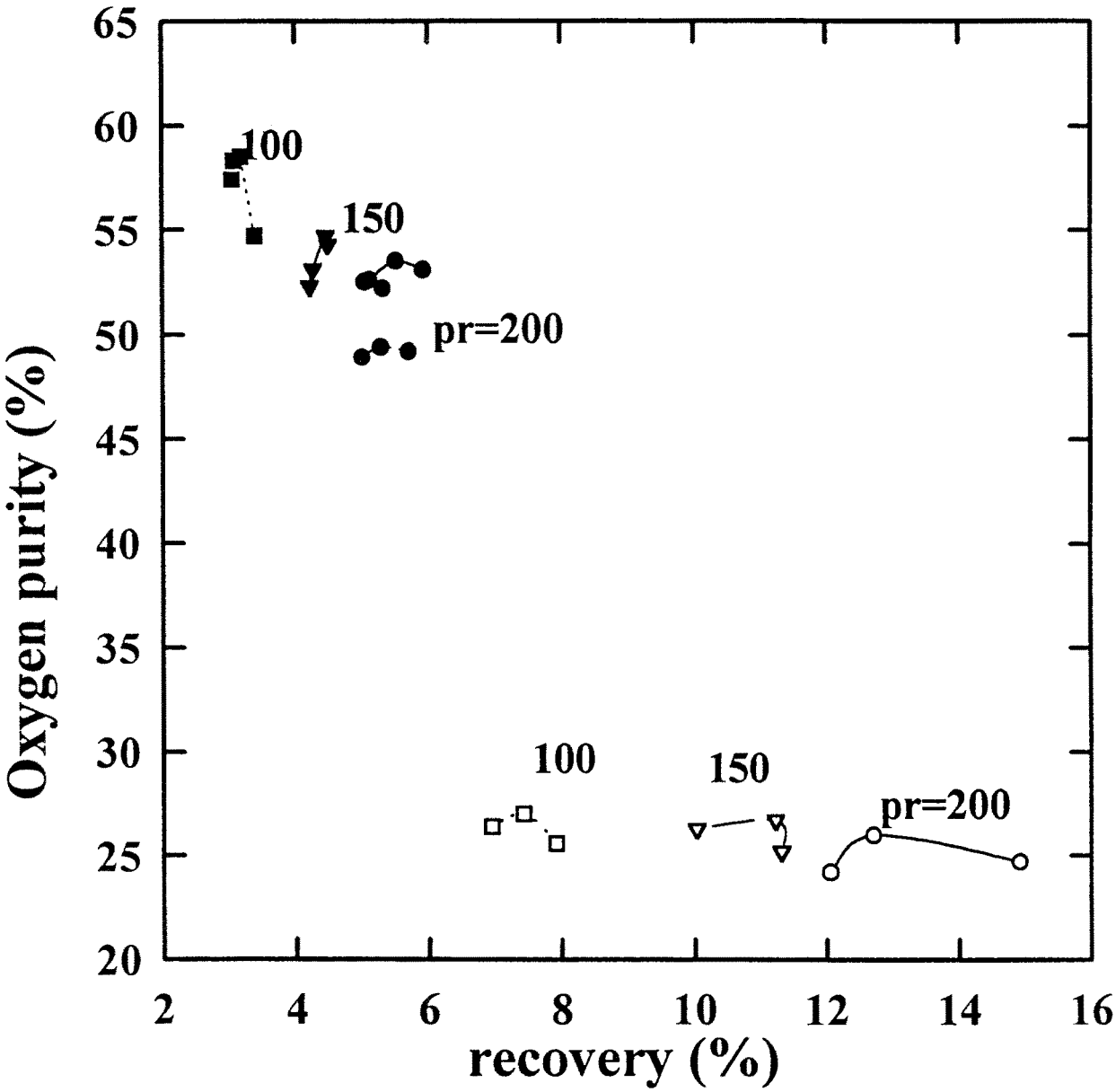

Fig. 7. The performance of the RFRPSA system packed with 3 μm 5A powder. The notations are the same as in Fig. 5.

drop could be estimated as followed. If we had doubled the packing radius without changing the total packing volume, the outer surface area would be reduced by half, and the overall pressure drop under the same feed rate would be about 2.6 times the original. On the other hand, for the same depth of feed penetration, a larger cross sectional area resulted into more solids experiencing the feed pressure. Consequently, more nitrogen would be adsorbed, and less gas would be passed down to the inner section. Based on this analysis, a 50% increase of particle size should be enough to balance the enlargement of radius, so that the same overall pressure drop could be maintained.

The experimental system studied have not fully realized the advantage of radial flow geometry, due to the difficulty of annualar packing. Estimation of pressure drop across a 10 cm disk of 3 μm particles based on

Table 1. Results of radial flow RPSA with 3 μm 5A zeolite powder packing under outward feed condition.

Cycle time (feed, delay, exhaust) (seconds)	Product purity (%)	Avg. feed rate (SLPM)	Production rate (SLPM)	Product end P (psig)	Surge tank P (psig)	Recovery (%)	Productivity of pure O_2 (SLPH/kg)
3, 2, 20	26.3	1.951	200	5 ~ 7	~6	12.89	5.3
2, 2, 20	27.4	1.883	200	4 ~ 6	~5	13.92	5.5
1, 2, 20	27.4	1.772	200	3 ~ 4	~3	14.79	5.5
0.5, 2, 20	25.8	1.499	150	2 ~ 3	~2	12.35	3.9
0.5, 2, 17.5	25.0	1.621	200	2 ~ 3	~2	14.76	5.0
1, 2, 20	26.3	1.753	200	4 ~ 5	~4	14.36	5.3
1, 1, 20	26.1	1.770	200	4 ~ 5	~4	14.11	5.2
1, 3, 20	26.0	1.677	200	5 ~ 6	~5	14.83	5.2
1, 2, 18	25.8	1.812	200	5 ~ 6	~5	13.63	5.2
1, 2, 22	26.1	1.710	200	3.5 ~ 4.5	~4	14.60	5.2
1, 2, 20	26.7	1.706	150	4 ~ 5	~4	11.23	4.0
1, 2, 20	27.0	1.742	100	5 ~ 6	~5	7.42	2.7
2, 2, 20	26.4	1.821	100	5 ~ 7	~6	6.94	2.6
0.7, 2, 20	25.6	1.545	100	2 ~ 4.5	~3.5	7.91	2.6
0.7, 2, 20	25.2	1.598	150	4 ~ 5	~4	11.32	3.8
2, 2, 20	26.3	1.880	150	6 ~ 7.8	~6.5	10.03	3.9
2, 2, 20	26.0	1.958	200	6 ~ 7.2	~6	12.71	5.2
3, 2, 20	24.2	1.921	200	6 ~ 9	~7	12.06	4.8
1, 2, 20	24.7	1.584	200	7 ~ 8	~6.5	14.92	4.9
4, 2, 20	24.6	1.815	200	2.5 ~ 5	~3	12.97	4.9
6, 2, 20	23.6	1.948	200	4 ~ 6.5	~5	11.59	4.7
5, 2, 20	23.2	1.862	200	4 ~ 7	~5	11.92	4.6

* Feed pressure 20 psig.
** total zeolite packed 600 gm.

Table 2. Results of radial flow RPSA with 3 μm 5A zeolite powder packing under inward feed condition.

Cycle time (feed, delay, exhaust) (seconds)	Product purity (%)	Avg. feed rate (SLPM)	Production rate (SLPM)	Product end P (psig)	Surge tank P (psig)	Recovery (%)	Productivity of pure O_2 (SLPH/kg)
3,1,10	52.5	9.982	200	5 ~ 10	~8	5.03	10.5
4,1,10	53.5	9.621	200	6 ~ 12	~10	5.32	10.7
5,1,10	52.2	9.410	200	7 ~ 14	~12	5.31	10.4
4,1,10	52.6	9.855	200	6 ~ 12	~10	5.11	10.5
4,1,12	53.5	9.290	200	5 ~ 12	~7.5	5.51	10.7
4,1,14	53.1	8.566	200	3 ~ 11	~4	5.93	10.6
3,1,12	52.3	8.912	150	4 ~ 10	~5	4.21	7.8
4,1,12	53.1	8.948	150	5 ~ 12	~6	4.26	8.0
5,1,12	54.7	8.809	150	5 ~ 14	~8	4.45	8.2
6,1,12	54.3	8.712	150	6 ~ 15	~9	4.48	8.1
3,1,12	58.1	9.034	100	4 ~ 10	~7	3.04	5.8
4,1,12	58.3	9.068	100	5 ~ 12	~8.5	3.07	5.8
5,1,12	58.5	8.826	100	6 ~ 14	~10	3.17	5.9
6,1,12	54.7	8.629	100	6 ~ 15	~10.5	3.03	5.5
4,0.5,12	48.9	9.368	200	4 ~ 12	~4	5.00	9.8
4,1,12	49.4	8.960	200	5 ~ 12	~4.5	5.28	9.9
4,2,12	49.2	8.253	200	5 ~ 12.5	~5	5.70	9.8
4,1,12	59.6	9.041	100	5 ~ 12	~7	3.15	6.0

* Feed pressure 20 psig.
** with the same packing as in Table 1.

Table 3. Comparison of literature data on axial flow RPSA processes with the results on radial flow RPSA system.

Data source	Jones & Keller (1981)			Pritchard & Simpson (1986)		Wu (1993)			Radial flow
Feed pressure (psig)	10.0	20.0	50.0	10.0		20.0	30.0	20.0	20.0
Adsorbent size (mesh)	40/80			60/80		60/80			3 μm
Packing depth (cm)	30.5	50.8	152.4	23.0	61.0	24.0	50.8	75.0	8.9
Product purity (%)	90.0	90.0	90.0	29.1	91.2	66.8	91.4	99.8	53.5
Oxygen recovery (%)	12.8	24.5	32.7	44.3	17.7	7.2	15.8	11.1	5.5
Productivity (mol pure O_2/Kg.day)	22.5	39.2	53.9	109.0	16.2	24.2	30.5	12.3	10.4
Feed time (second)	1.0	0.5	0.5	1.0	1.5	2.0	3.0	5.0	4.0
Delay time (second)	1.0	2.0	1.0	0.5	0.5	0.5	0.5	0.5	1.0
Exhaust time (second)	6.0	10.0	15.0	2.0	4.0	4.0	6.0	10.0	12.0

Blake Kozeny equation give values much larger than that observed. It suggests that channeling existed in our experimental system. This difficulty may be eliminated if, instead of an annular packing, a wedge shape packing was employed. Furthermore, if the forgoing argument is correct, an even larger effect shall be found in 3D geometry, i.e., packing the adsorbent into a hollow sphere. As before, we need not physically take the whole circumference of a sphere to cash its gain. A hemisphere or a cone section of sphere shall have all the expected benefit in theory.

Conclusions

When there was a significant pressure drop in a PSA process, the distribution of flow resistance became important to its performance. For a radial flow RPSA system, the inward feed operation always gave a better product purity than feeding from inside. This was attributed to a sharper pressure gradient near the center of the packing.

Two points distinguished a Radial Flow RPSA process from an axial one. First, particles as small as a few μm could be used directly, due to the larger cross sectional area and thus the smaller pressure drop in a radial flow geometry. The particle size employed here was about two orders of magnitude smaller than that commonly used in an axial RPSA process. A smaller particle size facilitated a faster adsorption kinetics, so that instantaneous equilibrium could be attained even under a very short cycle time.

The distribution of the flow resistance in radial flow and axial flow RPSA systems were different. Due to the change of cross sectional area, the flow resistance in RFRPSA was highest at the center, while it was almost evenly distributed in an axial flow system. Shifting the flow resistance down stream enabled a deeper feed penetration, and a higher adsorbent utilization. The desorption during vent step also became more effective. Therefore, for the same depth of packing, a Radial Flow RPSA process would be more effective than an axial flow RPSA. The Radial Flow RPSA process had a further benefit due to its geometry. More solids had chance to experience the large pressure swing on the feed side. Thus the system became more productive.

The performance of a RPSA process could have been improved by just increasing the flow resistance along the feed direction. This might be accomplished by decreasing the adsorbent particle size along column depth. Packing a column with specified particle size distribution would however be difficult. The RFRPSA system exemplified in this study have achieve the same goal by changing the flow area. The cross sectional area varied as $2\pi \cdot (R_e - d)$, where d was the distance from the feed end and R_e was the external radius of an annular disk. An even larger variation of cross section area was possible if the adsorbent had been packed into a right cylindrical cone, where the function would be $\frac{4}{3}\pi \cdot (R_e - d)^2$. Depending on the adsorption characteristics of the system, different functional form could be selected to optimize the distribution of flow resistance.

Acknowledgment

This study has been supported by the grand NSC-81-0402-E008-543 from National Science Council of ROC. The authors like to express thanks to Prof. T.Y. Lee for his mass flow controller.

References

Doong, S.J. and R.T. Yang, "The role of pressure drop in PSA," *Adsorp. and ion exchange: Fundam. and Appl.*, M.D. LeVan (Eds.), pp. 145–154, AIChE Symp. Ser., No. 264, **84**, 1988.

Jones, R.L. and G.E. Keller, US patent 4,194,892 (1980).

Jones, R.L. and G.E. Keller, "Pressure—Swing parametric pumping—a new adsorption process," *J. Sep. Proc. Technol.*, **2**, 17–23 (1981).

Keller, G.E. and R.L. Jones, "A new process for adsorption separation of gas mixture," *Adsorp. and ion exchange with synthetic zeolites*, W.H. Flank (Ed.), pp. 275–186, ACS Symp. Ser. No. 135, 1980.

Kowler, D.E. and R.H. Kadlec, "The optimal control of a periodic adsorber: Experiment and Theory," *AIChE J.*, **18**, 1207–1219 (1972).

Kumar, R., W.C. Kratz, D.E. Guro, D.L. Rarig, and W.P. Schmidt, "Gas mixture fraction to produce two high purity products by PSA," *Sep. Sci. Technol.*, **27**(4), 509–522 (1992).

Pritchard, C.L. and G.K. Simpson, "Design of an oxygen concentrator using the RPSA principle," *Chem. Eng. Res. Des.*, **64**, 467–471 (1986).

Rota, R. and P.C. Wankat, "Intensification of pressure swing adsorption processes," *AIChE J.*, **36**, 1299–1312 (1990).

Rota, R. and P.C. Wankat, "Radial flow pressure swing adsorption," Proc. *Adsorp. Proc. for gas sep.*, F. Meunier and M.D. LeVan (Eds.), pp. 143–148, GFGP, Nancy, France, 1991.

Turnock, P.H. and R.H. Kadlec, "Separation of nitrogen and methane via periodic adsorption," *AIChE J.*, **17**, 335–342 (1971).

Wu, S.T., MS thesis, National Central Univ. Taiwan ROC (1993).